The impact of GPS receiver modifications and ionospheric activity on Swarm baseline determination

Mao, X.; Visser, P. N.A.M.; van den IJssel, J.

Important note
To cite this publication, please use the final published version (if applicable).
Please check the document version above.

Accepted Manuscript

The impact of GPS receiver modifications and ionospheric activity on Swarm baseline determination

X. Mao, P.N.A.M. Visser, J. van den IJssel

The impact of GPS receiver modifications and ionospheric activity on Swarm baseline determination

X. Mao[a,*], P.N.A.M. Visser[a], J. van den IJssel[a]

[a]Delft University of Technology, Kluyverweg 1, 2629 HS Delft, The Netherlands

Abstract

The European Space Agency (ESA) Swarm mission is a satellite constellation launched on 22 November 2013 aiming at observing the Earth geomagnetic field and its temporal variations. The three identical satellites are equipped with high-precision dual-frequency Global Positioning System (GPS) receivers, which make the constellation an ideal test bed for baseline determination. From October 2014 to August 2016, a number of GPS receiver modifications and a new GPS Receiver Independent Exchange Format (RINEX) converter were implemented. Moreover, the on-board GPS receiver performance has been influenced by the ionospheric scintillations.

The impact of these factors is assessed for baseline determination of the pendulum formation flying Swarm-A and -C satellites. In total 30 months of data - from 15 July 2014 to the end of 2016 - is analyzed. The assessment includes analysis of observation residuals, success rate of GPS carrier phase ambiguity fixing, a consistency check between the so-called kinematic and reduced-dynamic baseline solution, and validations of orbits by comparing with Satellite Laser Ranging (SLR) observations. External baseline solutions from The German Space Operations Center (GSOC) and Astronomisches Institut - Universität Bern (AIUB) are also included in the comparison.

Results indicate that the GPS receiver modifications and RINEX converter changes are effective to improve the baseline determination. This research

---

*Corresponding author; Tel.:+31 (0)15 27 82065; Fax:+31(0)15 27 82072
    Email address: x.mao@tudelft.nl (X. Mao)

eventually shows a consistency level of 9.3/4.9/3.0 mm between kinematic and reduced-dynamic baselines in the radial/along-track/cross-track directions. On average 98.3% of the epochs have kinematic solutions. Consistency between TU Delft and external reduced-dynamic baseline solutions is at a level of 1 mm level in all directions.

Keywords: Precise Baseline Determination, Swarm Satellite, Ionospheric Scintillation, GPS Receiver Modifications, Antenna Patterns

1. Introduction

The Swarm mission, launched on 22 November 2013, is the fifth mission of the European Space Agency (ESA) living planet program. With three identical satellites, Swarm aims at unscrambling the Earth geomagnetic field and its
5 temporal variations [1]. In its scheduled mission timetable, various maneuvers are made to guarantee a detailed coverage of the Earth [2], both in spatial and temporal resolution. After the early orbit commissioning phase, the Swarm-A and -C satellites fly in orbital planes with the same inclination, but a difference of $1.5°$ in right ascension of ascending node and about $0.3° - 0.9°$ in argument
10 of latitude. These differences manifest themselves as a pendulum like relative motion [1]. Swarm-B is flying in a higher and different polar orbit.

A few formation flying satellite missions have been launched in the past years. Their different baseline types enable various research objectives. The in-line formation flying GRACE and its follow-on mission focus on the research of
15 the Earth's gravity field and its variations [3]. The side-by-side flying TanDEM-X/TerraSAR-X mission (baseline of just a few kms) aims at constructing global digital elevation models by the interferometric synthetic aperture radar technique [4]. The PRISMA mission intends to investigate rendezvous and docking in space [5, 6]. Compared to these missions, the Swarm-A and -C formation has
20 a unique pendulum-type baseline. If precisely determined, this baseline could be an ideal test bed for investigating gravity field recovery by making use of baseline perturbations in the cross-track direction [7].

The three Swarm satellites are equipped with the *RUAG space* dual-frequency, high-precision, eight-channel GPS receivers, which facilitate both single-satellite
²⁵ Precise Orbit Determination (POD) and dual-satellite Precise Baseline Determination (PBD) [8]. The GPS receiver satellite-to-satellite tracking observations are affected by the local environment in which the constellation flies and the GPS signal travels. Much research has proved the significance of using in-flight data derived antenna Phase Center Variation (PCV) and Code Residual Variation
³⁰ (CRV) patterns. Using these patterns for correcting the GPS observations enhances the POD and PBD performance [9, 10, 11, 12, 13, 14, 15, 16]. At present 2 cm precision level is achievable for Swarm POD solutions [12], and 1-2 cm consistency level is obtained between Swarm-A/-C kinematic and reduced-dynamic PBD solutions [17].

³⁵ Ionospheric scintillations have a big impact on the performance of Swarm GPS receivers and moreover POD [12] and PBD [14]. Irregular ionospheric plasma bubbles and thunderstorms cause GPS tracking losses near the equator. Strong solar winds will downgrade the GPS receiver tracking capability near the two geomagnetic poles [18, 19]. To minimize ionospheric influences in these
⁴⁰ geographical areas and to improve the GPS signal tracking performance, modifications have been made to the Swarm GPS receivers from October 2014 to August 2016, as depicted in Table 1. On 11 April 2016, a software issue in the RINEX converter was fixed that caused high noise in the code range observations contained in the Swarm GPS products (https://earth.esa.int/web/guest/news/-
⁴⁵ /article/swarm-software-issue-in-rinex-converter-fixed). GPS receiver modifications, especially the improved carrier phase Tracking Loop (TL) bandwidth and increased antenna Field-of-View (FoV), are proved to be effective in improving the POD [20]. More importantly, it has been shown that gravity field recovery which relies on kinematic POD solutions, also benefits from the applied GPS
⁵⁰ receiver modifications [21].

In this research, we focus on analyzing the impact of ionospheric activity and Swarm GPS receiver modifications on PBD. It is crucial for the users of the Swarm GPS data to note the impact of these factors on the data quality in

3

different periods. In total 30 months of the lower pair Swarm-A and -C satellites
₅₅ data (from 15 July 2014, when two GPS receivers started to track 1 Hz data,
to the end of 2016) are selected to investigate the influence of the ionospheric
activity and GPS data quality. The days without either reference orbits or GPS
RINEX files are first excluded, and the days with large maneuvers (7 days for
Swarm-A, 1 day for Swarm-C) and data gaps are also not analyzed. An overview
₆₀ of all Swarm satellites maneuvers is available in this report [22].

Table 1: Swarm GPS receivers modifications and the RINEX converter change timetable during the entire period.

Date	Modifications
15-07-2014	GPS data rate 0.1 Hz to 1 Hz
21-10-2014	Swarm-A FoV 80° to 83°
22-10-2014	Swarm-B/-C FoV 80° to 83°
01-12-2014	Swarm-C FoV 83° to 86°
13-01-2015	Swarm-C FoV 86° to 88°
06-05-2015	Swarm-A/-B FoV 83° to 88°
06-05-2015	Swarm-C TL L1C+50%,L2W+100%,C1W/C2W+100%
08-10-2015	Swarm-A TL L1C+50%,L2W100%,C1W/C2W+100%
10-10-2015	Swarm-B TL L1C+50%,L2W+100%,C1W/C2W+100%
11-04-2016	New RINEX converter
27-04-2016	Swarm-B code TL to original setting
03-05-2016	Swarm-A code TL to original setting
04-05-2016	Swarm-C code TL to original setting
23-06-2016	Swarm-C phase TL L2W+50% (0.5 Hz to 0.75 Hz)
11-08-2016	Swarm-A phase TL L2W+50% (0.5 Hz to 0.75 Hz)
11-08-2016	Swarm-C phase TL L2W+50% (0.75 Hz to 1.0 Hz)

The Swarm GPS receiver carrier phase observation has tremendously lower
noise level than pseudo-range/code observation [12]. As a prerequisite of mak-
ing optimal use of carrier phase in PBD, the so-called Double-Differenced (DD)

4

integer ambiguities should be fixed. However the Swarm GPS receivers expe-

65   rience a mixture of half-cycle and full-cycle ambiguities because of the applied
tracking methods [17]. It has to be taken into consideration, otherwise only
fixing the integer ambiguities as full-cycles significantly downgrades the PBD
[14, 7]. Swarm lacks an independent baseline validation system, e.g. the K-band
ranging system on-board the GRACE twin-satellites. Therefore for Swarm we

70   have to verify the baseline precision by other means. An alternative validation
is the consistency check between the reduced-dynamic and the kinematic PBD,
which is solely determined by the GPS receiver observation quality [23]. The
ambiguity fixing success rate is another verification, however it has to be noted
that wrongly fixed ambiguities might pass the validation scheme.

75   This paper is organized as follows. The POD and PBD methodology is
outlined in Section 2. Special attention is paid to the fixing and validation of
the half-cycle integer ambiguities. The POD and PBD is based on an iterative
Extended Kalman Filter (EKF), where the GPS observations are treated sepa-
rately for the two GPS frequencies. The EKF computes the reduced-dynamic

80   POD and then kinematic and reduced-dynamic PBD, where for PBD relative
dynamics between two satellites can be additionally constrained. In Section 3,
the in-flight performance of the GPS receivers is addressed and analyzed. The
internal ambiguity fixing success rate, observation residual levels and the con-
sistency of different baseline solutions are checked. POD and PBD solutions in

85   this study are compared with independent Satellite Laser Ranging (SLR) ob-
servations. External PBD solutions from The German Space Operations Center
(GSOC) [14, 17] and Astronomisches Institut - Universität Bern (AIUB) [7] are
also used for comparison. Finally, Section 4 concludes this paper and proposes
a few research perspectives.

5

2. Precise baseline determination methodology

2.1. Integer ambiguities fixing and validation

The GPS carrier phase observations offer the most crucial information for computing precise baselines. When constructing the DD observation model between two GPS receivers and two GPS satellite transmitters, a few common errors such as GPS clock and ephemeris errors can almost be eliminated or reduced to a large extent. By fixing as many DD carrier phase integer ambiguities as possible, the EKF is able to fully exploit the carrier phase precision. In this research, the implemented ambiguities fixing algorithm is Least-squares Ambiguity De-correlation Adjustment (LAMBDA), which is proved to be very successful for the determination of static baselines on the ground [24] and dynamic baselines in space [23].

It has to be noted that the Swarm GPS receivers experience half-cycle ambiguity, which makes ambiguity fixing more challenging. The half-cycle ambiguity is caused by the fact that the Swarm GPS receiver Numerically Controlled Oscillator (NCO) phase and the derived carrier phase observation may be affected by 180 degrees phase offset for an individual GPS-Swarm pass [17]. [14] designed a filter to distinguish between the half-cycle and the full-cycle ambiguities and fixed them separately. In their research, the solution fixing mixed-cycle integer ambiguities obtained 3.9% more integer ambiguities than the solution fixing all ambiguities as half-cycle values. Besides, in [17] they selected day 29 February 2016 as a test case and the mixed-cycle solution resulted in a slightly better baseline consistency from 5.02 to 4.87 mm in the along-track direction. The cost was 2-2.5 times more processing time. They also corrected all the half-cycle ambiguities to full-cycle values, which contributed much to the ambiguity fixing process. When using the ESA RINEX data in this research, all GPS DD carrier phase ambiguities are fixed as half-cycle values.

To maximize the ambiguity fixing success rate, a subset fixing process is implemented. The LAMBDA algorithm aims at making optimal use of float ambiguities and the associated covariance matrix as computed by the EKF

6

120 for fixing the ambiguities at integer values [23]. The conventional use of the LAMBDA algorithm has a drawback that none of the ambiguities will be accepted for epochs for which one or more of the fixed ambiguities can not pass the statistical testing. To avoid this, a subset selection approach is adopted leading to many more fixed ambiguities [25].

125 To begin with, a GPS satellite with the smallest ambiguity variance is selected as the reference. If LAMBDA fails to fix the full set of ambiguities, a subset selection approach will be used. It discards the least likely fixed ambiguities as provided by LAMBDA but fail to pass the ambiguities validations. The subset selection repeats until LAMBDA fixes a smaller subset. The fixed

130 subset ambiguities are then fed into the next EKF iteration to further fix the discarded set of ambiguities. Figure 1 depicts the ambiguity fixing process of an epoch. It can be seen that eventually five pairs of ambiguities are fixed after six iterations by using this subset fixing approach, however the G28-G05 pair remains un-fixed. Please note that three of the five fixed ambiguities have

135 odd values, which indicate that they are half-cycle ambiguities. Moreover, a rather strict statistical testing is conducted to check the validity of the fixed ambiguities (Section 3.2).

Figure 1: The subset ambiguities fixing (on the first GPS frequency) for a representative epoch, 00:30:00 on 17 July 2014 (DOY 198). The horizontal axis represents the consecutive EKF iterations, the vertical axis indicates the pair of GPS satellites for forming the double-differenced ambiguities.

7

2.2. Multiple Orbit Determination using Kalman filtering

This research is accomplished by using a GPS High Precision Orbit Deter-
mination Software Tools (GHOST) add-on tool called Multiple Orbit Determi-
nation using Kalman filtering (MODK) [25]. GHOST is a precise orbit deter-
mination software package developed by GSOC with support from TU Delft
[26].

The satellite dynamic modeling consists of three parts: gravitational forces,
non-gravitational forces and empirical accelerations. Empirical accelerations
are the estimated parameters to compensate force model errors. In the EKF,
the correlation time (τ), the standard deviation of a-priori values (σ_a) and the
process noise (σ_p) of empirical accelerations have to be set. The implemented
models, used data files and EKF settings are specified in Table 2. It can be
observed that a comprehensive modeling of gravitational forces is done, includ-
ing the GOCO03S gravity field model truncated at degree and order 120, ocean
tides and 3rd-body perturbations. The modeling of non-gravitational forces is
based on a simplified canon-ball modeling of the satellites. Associated modeling
errors are compensated by the estimation of atmospheric drag (C_D) and solar
radiation (C_R) coefficients, and the estimation of empirical accelerations. Since
the Swarm-A and -C satellites are flying in adjacent orbits, it is anticipated
that the associated force model errors, which are to be absorbed by the empir-
ical accelerations, are quite similar. Therefore, in PBD differential acceleration
constraints are applied that cause the estimated empirical accelerations to be
similar as well for both Swarm satellites.

The detailed filtering process in MODK is illustrated in Figure 2. MODK
includes both a forward and backward filter and iterates until convergence. The
EKF first runs from the first epoch to the last epoch of each 24-hours orbit arc
with 5 s step. For each epoch, the covariance matrix of the estimated parame-
ters is recorded. The estimated float integer ambiguities and the corresponding
covariance matrices are used by the LAMBDA algorithm in order to fix the
maximum number of integer ambiguities (subset approach). This process is re-
peated in the backward direction from the last to the first epoch. Subsequently

8

Table 2: Overview of MODK input template for the baseline determination of Swarm.

Spacecraft model	Canon-ball with cross-section of 1.0 m^2 and varying mass
Gravitational forces	GOCO03S 120×120 (selectable, maximum 250×250) static gravity field, plus linear trends for spherical harmonic degree 2 terms according to IERS2003 [27, 28]
	Luni-solar third body perturbations
	CSR Ocean tides model based on TOPEX and GRACE data [29]
Non-gravitational forces	Atmospheric drag: Jacchia 71 density model [30]
	Solar radiation pressure: conical Earth shadow, Sun flux data
C_D	1 per 24 hr, $\sigma_a = 1.3$, $\sigma_p = 1.0$
C_R	1 per 24 hr, $\sigma_a = 1.3$, $\sigma_p = 0.5$
Empirical acc.	Radial : $\tau = 600$ s, $\sigma_a = 5$ nm/s^2, $\sigma_p = 1$ nm/s^2
	Along-track: $\tau = 600$ s, $\sigma_a = 15$ nm/s^2, $\sigma_p = 3$ nm/s^2
	Cross-track: $\tau = 600$ s, $\sigma_a = 15$ nm/s^2, $\sigma_p = 3$ nm/s^2
Differential empirical acc.	Radial : $\tau = 600$ s, $\sigma_a = 2$ nm/s^2, $\sigma_p = 0.2$ nm/s^2
	Along-track: $\tau = 600$ s, $\sigma_a = 5$ nm/s^2, $\sigma_p = 1$ nm/s^2
	Cross-track: $\tau = 600$ s, $\sigma_a = 5$ nm/s^2, $\sigma_p = 1$ nm/s^2
Earth parameters	Leap second data table of TAI-UTC
	CODE Earth rotation parameters, version 2.0 [31]
GPS products	CODE 5s GPS orbits and clocks [32]
	IGS08.atx, the transmitter antenna phase center offsets and variations [33]
	CODE ionospheric maps [34]
GPS data editing	Minimum signal to noise ratio [-] : 5
	Minimum cut-off elevation [deg] : 0
	Code editing outliers [m] : 2.0
	Phase editing outliers [m] : 0.02
Orbit arc length	24 hours
Antenna pattern	Frequency-dependent phase and code antenna patterns
Ambiguity	Half-cycle Integer ambiguities
Methodology	Iterative Extended Kalman filter
GPS data weighting	For POD: Code/Phase: 0.3/0.003 [m]
	For PBD: Code/Phase: 0.5/0.005 [m]

9

the estimated integer ambiguities derived from the two directions are compared.
In case of consistent values for the forward and backward directions, the ambiguities are considered to be fixed. The EKF smooths both solutions according to the bi-directional covariance matrices recorded at each epoch. In the next iteration, the smoothed orbit and fixed ambiguities are set as input and it is attempted to fix more ambiguities. Iterations are repeated until no new integer ambiguities are fixed.

After the convergence of the reduced-dynamic baseline, a kinematic baseline solution is produced as well using the least squares method. To this aim, the same frequency-dependent GPS observations and fixed integer ambiguities on the two frequencies are used, where one satellite (Swarm-A) is kept fixed at the reduced-dynamic PBD solution. At least 5 observations are required on each frequency to form good geometry. To minimize the influence of wrongly fixed ambiguities and residual outliers, a threshold of 2-sigma of the carrier phase residual standard deviation statistics is set, which results in eliminating around 5% data. A further screening of 3 cm is set to the Root-Mean-Square statistics of the kinematic PBD carrier phase observation residual. It is able to screen out the solutions influenced by large wrongly fixed ambiguities and bad phase observations [23]. The kinematic PBD also runs bi-directional and two solutions are averaged according to the epoch-wise covariance matrices from the least squares method.

3. Results and discussion

3.1. GPS data processing

The Swarm Level-1B GPS observations are not recorded at integer seconds and need to be synchronized to exactly the same integer epochs for each Swarm satellite to facilitate the PBD. The approach as outlined in [12] is adopted, which synchronizes the different Swarm clocks to within 0.3 μs. A few GPS data editing thresholds are defined for the signal to noise ratio, elevation cutoff angle and code/phase observation detection outliers, as indicated in Table 2.
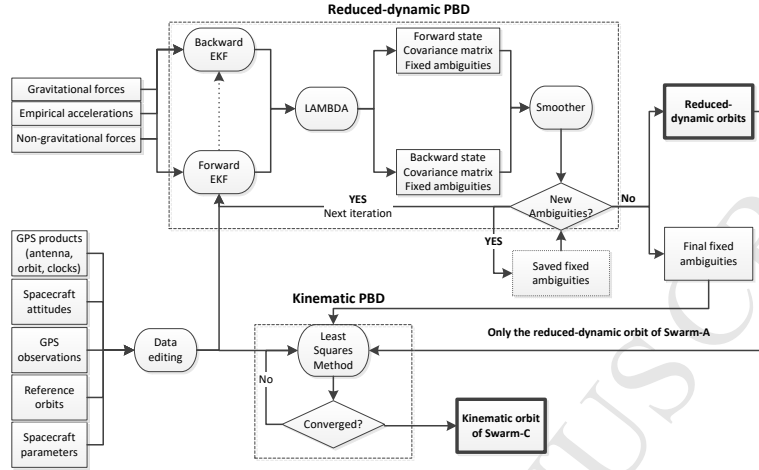
10

Figure 2: Flow chart of the iterative Extended Kalman filter and ambiguities fixing for reduced-dynamic baseline determination, and the Least Squares Method for kinematic baseline determination.

This editing scheme is applied for the full Swarm data period. The percentage of remaining data used in this study is shown in Figure 3.

Figure 3 agrees well with results included in [20]. It is found that the number of tracked GPS satellites by each receiver increases with larger antenna FoV and wider signal tracking loop bandwidth. For two satellites, the 80° to 88° FoV change leads to an increase of the average number from 7.3 to 7.5. In addition, the first tracking loop modification then leads to further increase to 7.7. When this modification was switched back to its original setting on 3 May 2016 and 4 May 2016 for Swarm-A and -C respectively, the number decreased again. However it has to be noted that the FoV changes to Swarm-A and -C are not synchronized: the nominal change always begins with Swarm-C. The number of simultaneously tracked GPS satellites by two receivers is influenced when the two Swarm satellites have different FoVs. The number drops from 7.2 (July to October 2014, the FoVs were 80°) to merely 6.2 (February to May 2015, the FoV of Swarm-A was 83° and -C had 88°), which leads to fewer available DD
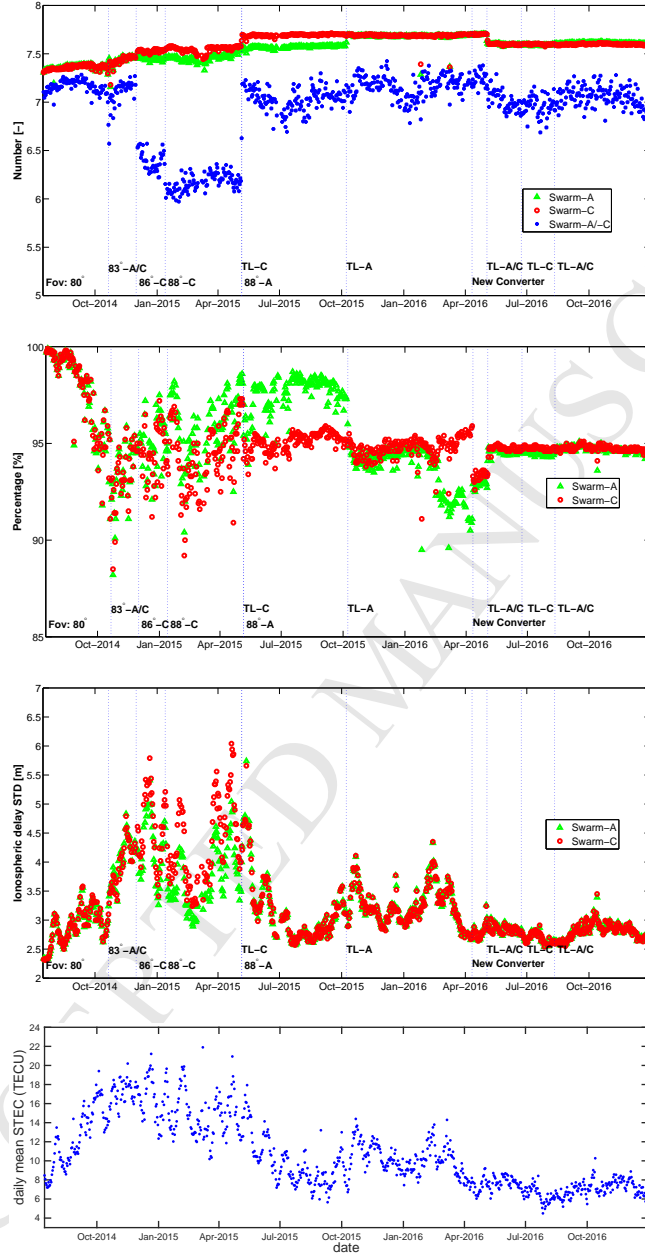
11

Figure 3: From top to bottom: the number of tracked GPS satellites by two GPS receivers, the percentage of used GPS data for two satellites in precise baseline determination, the standard deviation of the un-differenced ionospheric delay estimated in Kalman filter, and the daily mean values of STEC from the Swarm-C ESA level-2 TEC product.

12

integer ambiguities for PBD. When both antennas have the same 88° FoV, this number is close to 7.0.

₂₁₅ The Swarm GPS receivers are able to track the GPS L1-C/A signal and the encrypted P(Y) signals. Five main ranging observation types are three code/pseudo-range observations marked as C1C, C1W and C2W, and two carrier phase observations indicated as L1C and L2W [35]. Moreover, we find that the tracked C1C observations show higher noise levels than the C1W data, and it ₂₂₀ is thus more difficult to fix integer ambiguities for the C1C and L1C code/phase observations combination. Therefore, use will be made of the C1W observations for the code observation on the first GPS frequency for this study.

The GPS observation quality is influenced by the level of ionospheric activity including irregular scintillations, plasma bubbles and storms. Moreover, solar ₂₂₅ activity approached its 11 years peak level at the end of 2014, which is reflected by the Slant Total Electron Content (STEC) level in Figure 3. This effect can be also observed by the EKF estimation of the daily standard deviation of ionospheric delays between a Swarm satellite and the tracked GPS satellites. A larger ionospheric activity level in the winter of 2014 reduces the percentage of ₂₃₀ kept data from around 99% to below 95% in PBD, reminding that the same data editing scheme as described in Table 2 is used for the full analyzed Swarm data period. The first tracking loop modification of Swarm-C improves the number of available GPS observations, but it is found that the additional observations mostly experience larger thermal noise levels. Therefore, approximately 3% ₂₃₅ more data is eliminated and not used in PBD, which is comparable to the increment of observations due to the receiver modification. It has to be noted that there was a drop of selected data again during 21 February - 10 April, 2016, when the Swarm RINEX converter issue was causing a huge increase in the code observation noise of Swarm-A (Figure 4).

₂₄₀ Figure 4 illustrates the code/phase residual levels on each frequency after the data editing. The carrier phase experiences different residual levels on two frequencies, which are due to the different tracking methods applied for the L2-P(Y) and L1-C/A signals in the Swarm GPS receivers [17]. The GPS receiver
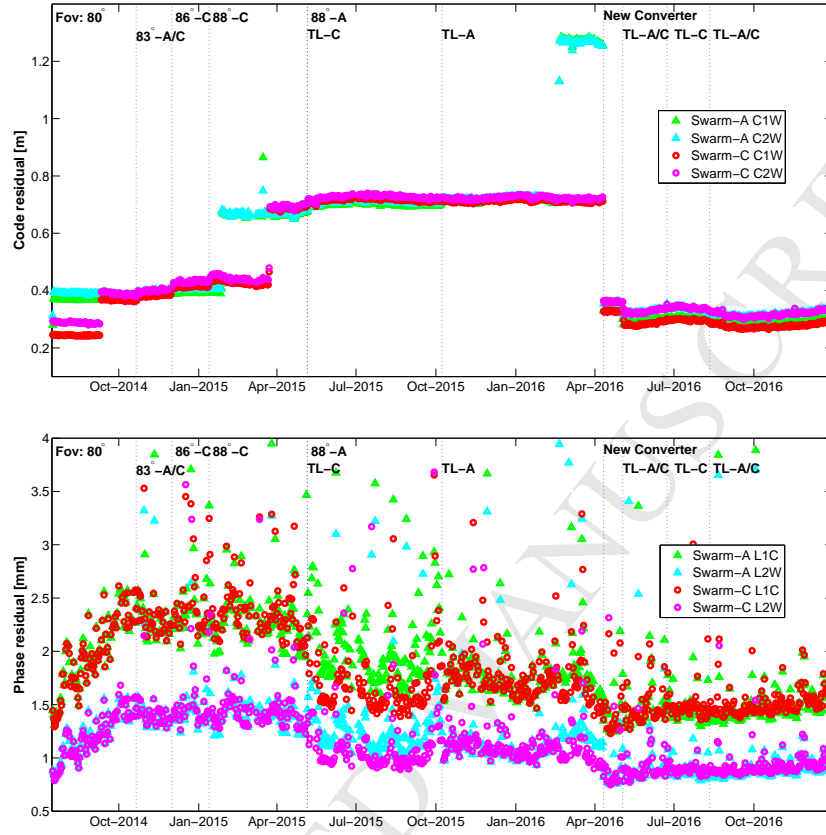
13

Figure 4: The code (top) and phase (bottom) residual levels on each frequency during the entire period.

modifications affect the observation quality in the following aspects:

²⁴⁵ • the larger FoV slightly increases the code and phase residuals, as reported by [20].

- the software issue with the old RINEX converter resulted in larger code residuals, and this was eventually solved on 11 April 2016 when the new RINEX converter was implemented.

²⁵⁰ • the first tracking loop modification (in May 2014) impacts the phase observations more than the other two modifications (in May 2016 and Au-

14

gust 2016, respectively). When this modification is first implemented on Swarm-C, it experiences clearly lower phase residuals than Swarm-A. This is mostly caused by the significant observation residual reduction near the
255 geomagnetic poles, where the large influence from ionospheric scintillations is reduced [20]. This reduction is larger than the slight thermal noise increment of GPS observations due to its widened tracking loop bandwidth. This is consistent with the discussion for Figure 3.

- the influence of GPS receiver modifications on code observation is quite
260 limited, because the RINEX converter software issue increases the residual level. Moreover we are using a strict data editing scheme to ensure good PBD environment, the larger-residual code observations are partially neglected in PBD (Figure 3).

- the carrier phase residuals are highly determined by the level of ionospheric
265 activity. They fluctuate accordingly when comparing with the STEC trend and the standard deviation of ionospheric delay estimates (Figure 3). The activity level is reduced significantly from 2014 to 2016 for both satellites.

After the implementation of new RINEX converter and three GPS receiver tracking loop modifications, the ionospheric activity is also low, therefore both
270 the phase and code residuals have been at low level for 7 months from May to December 2016.

Moreover, PCV and CRV maps have been estimated by the so-called *residual approach* [36]. These maps are used to correct the GPS observations and therefore to enhance the PBD method [14, 25]. To minimize the disturbance
275 from the RINEX converter issue, four representative months of data (August 2014, November 2014, August 2016 and November 2016) are selected for estimating the antenna maps. Compared with [37] and [17] which make use of the differential antenna patterns between two GPS receivers, this research estimates the antenna patterns of two receivers separately. Because the ambiguity
280 fixing is frequency-dependent, the relevant antenna pattern maps are created

15

for each GPS frequency (L_1 and L_2) in single satellite POD. Five iterations are found to be sufficient to first create the PCV maps, then another five iterations are done to further create the CRV maps based on a fixed PCV map. The detailed frequency-dependent PCV and CRV maps of Swarm-A are displayed

285 in Figure 5. The maps are defined in a right-handed North-East-Up (NEU) antenna-fixed reference system, for which the North axis coincides with the satellite body-fixed +X axis (0° azimuth), the Up and bore-sight axis coincides with the -Z axis, and the East axis completes the right-handed system. The Swarm-C GPS receiver experiences nearly identical patterns.

290 *3.2. Internal consistency check*

Ten representative days from different periods are selected to depict how the iterative approach gradually increases the PBD integer ambiguity fixing success rates in Figure 6. In general, 5 iterations are sufficient to converge the PBD. After May 2016, the ambiguity fixing becomes more efficient as the first

295 iteration fixing success rate is higher and eventually more ambiguities can be successfully fixed in fewer iterations. The impact of GPS receiver modifications and ionospheric activities on the integer ambiguities fixing success rate is displayed in Figure 7. Here an ambiguity probability test with threshold of 99.9% is adopted. The complete set of validations is described in [25]. It is quite

300 strict to avoid wrongly fixed ambiguities and thus ensure stable kinematic and reduced-dynamic baselines. The best integer ambiguities fixing success rate at around 90% is achieved during 15 July 2014 - 1 September 2014. For this period both the code and the phase residual levels are relatively lower and most of the observations can be used for PBD. After this period, the ambiguity fixing

305 success rate decreases when the code residual noise level increases because of the RINEX converter issue and the phase residual noise level increases because of larger ionospheric activity. The lowest success rate occurs when the code residual noise level for the Swarm-A GPS receiver is at a peak near April 2016 (Figure 4), although for this period the influence of ionospheric activity is low.

310 This indicates that the code observation noise level is also an important impact
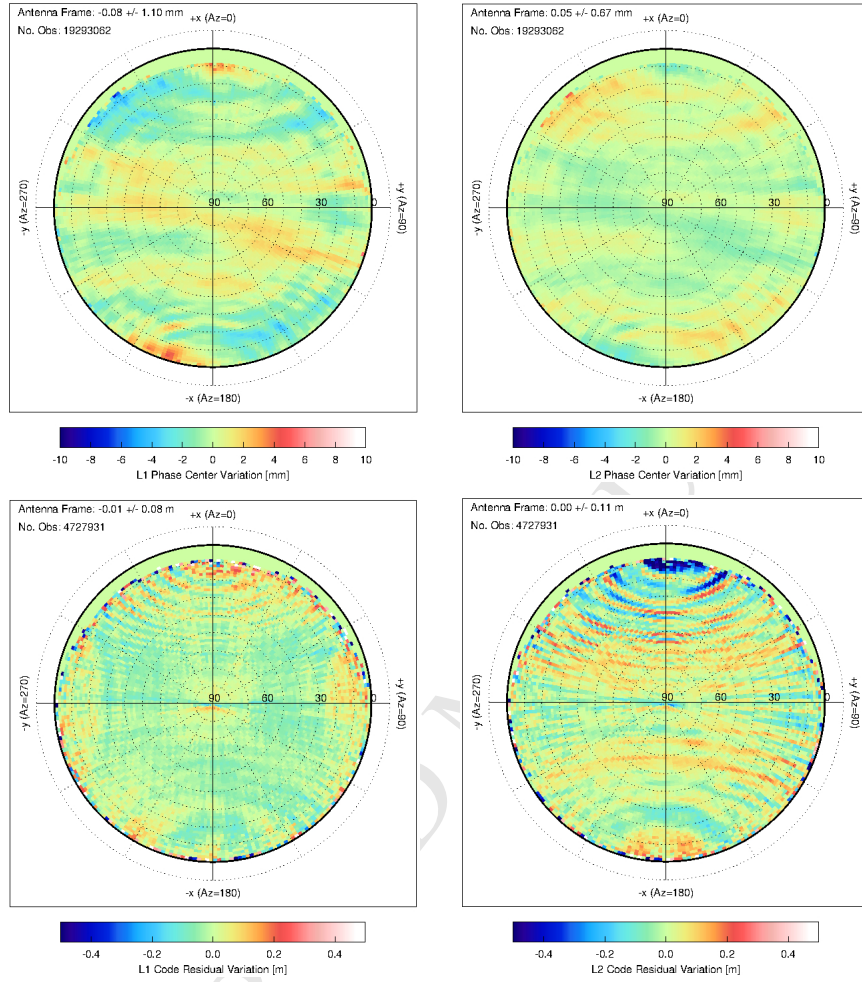
16

Figure 5: The in-flight PCV (top) and CRV (bottom) maps of Swarm-A: L_1 frequency (left) and L_2 frequency (right) in the NEU reference frame (four months data).

factor in fixing the integer ambiguities.

Figure 8 displays the global distribution of the Swarm-A carrier phase residuals for the L_1 frequency. The distributions are clearly different for the month of August in 2014 and 2016. For August 2014, much stronger residuals are witnessed near especially the geomagnetic poles. This is highly correlated with ionospheric scintillations. For August 2016, the residual level at the poles is much lower. This can be attributed to two important factors: (1) GPS receiver
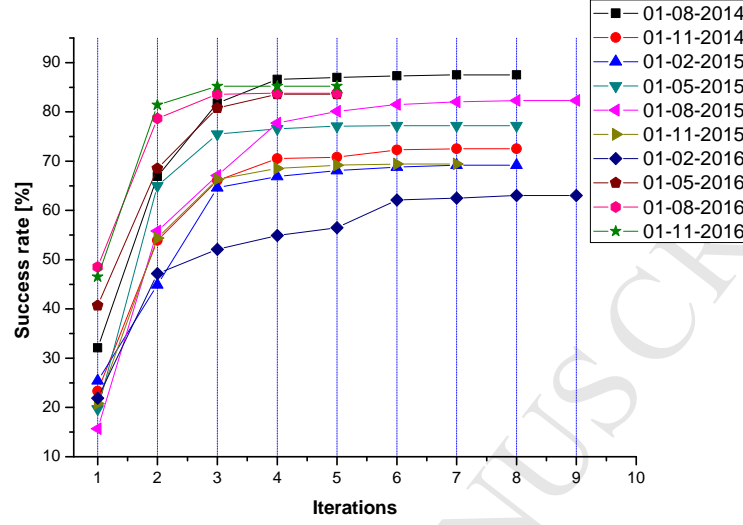
17

Figure 6: Ambiguities fixing success rate against iterations for 10 representative days.
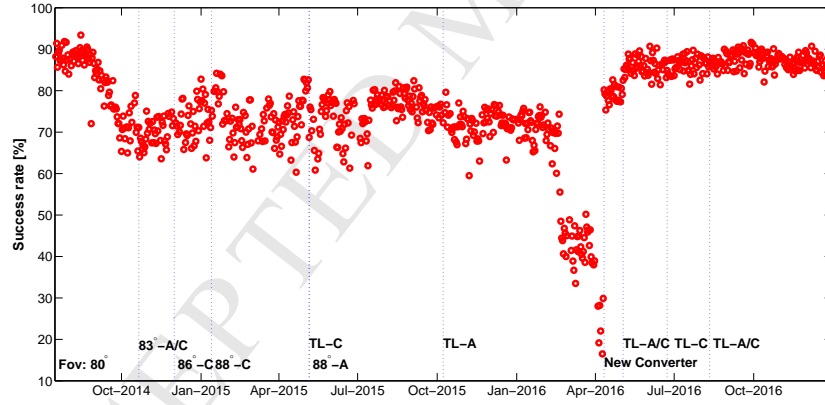
Figure 7: Ambiguities fixing success rate during the full period.

modifications enhance the tracking performance at the poles, and (2) the ionospheric activity level decreases from 2014 to 2016. However, when comparing the residual levels for middle-latitude areas, the phase residuals slightly increase from 2014 to 2016. This is caused by the increased phase tracking loop bandwidth and antenna FoV which provide more data tracked at lower elevations.
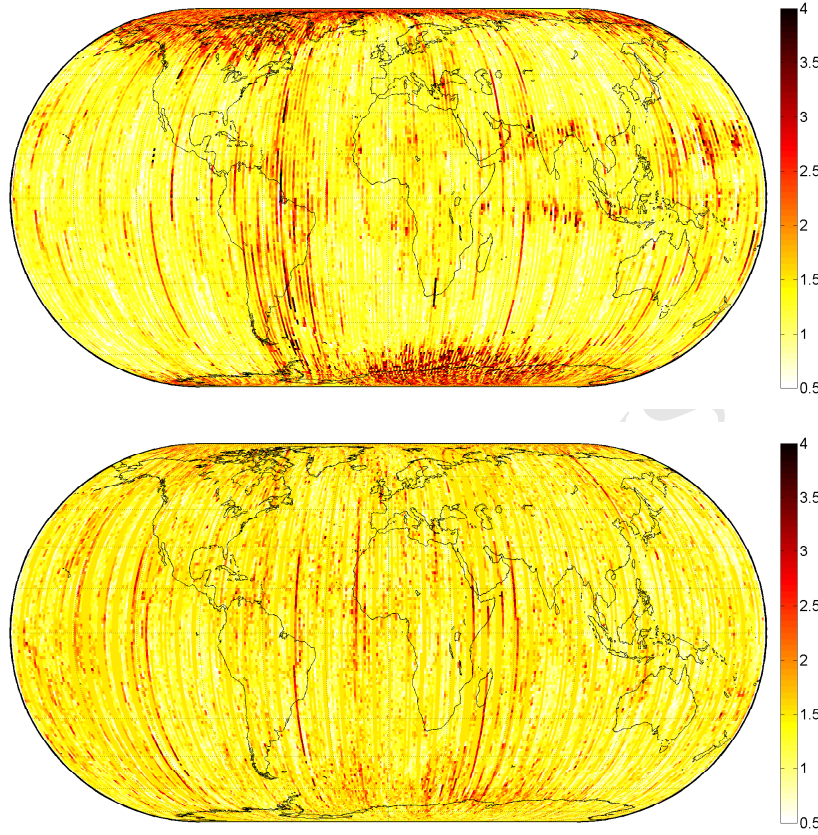
18

Figure 8: The global distribution of the L_1 frequency phase residuals of Swarm-A satellite in August 2014 (top) and August 2016 (bottom), unit: [mm].

These additional observations are slightly more noisy.

The consistency between the kinematic and the reduced-dynamic baselines is used to assess the quality of the PBD process [14, 7]. In this research, both approaches rely on the same GPS observations and fixed integer ambiguities. The kinematic approach solely exploits GPS observations in a batch least-squares filter, while the reduced-dynamic approach uses a Kalman filter that relies on the dynamic modeling of satellites together with the estimation of empirical accelerations. To maximize the availability of kinematic baselines, the adopted approach uses all available fixed integer ambiguities and if not uses the float

19

ambiguities. No kinematic solutions are computed for epochs with fewer than 5 simultaneously tracked GPS satellites by the two Swarm GPS receivers after the 3 cm screening in the kinematic PBD, as mentioned in Section 2.
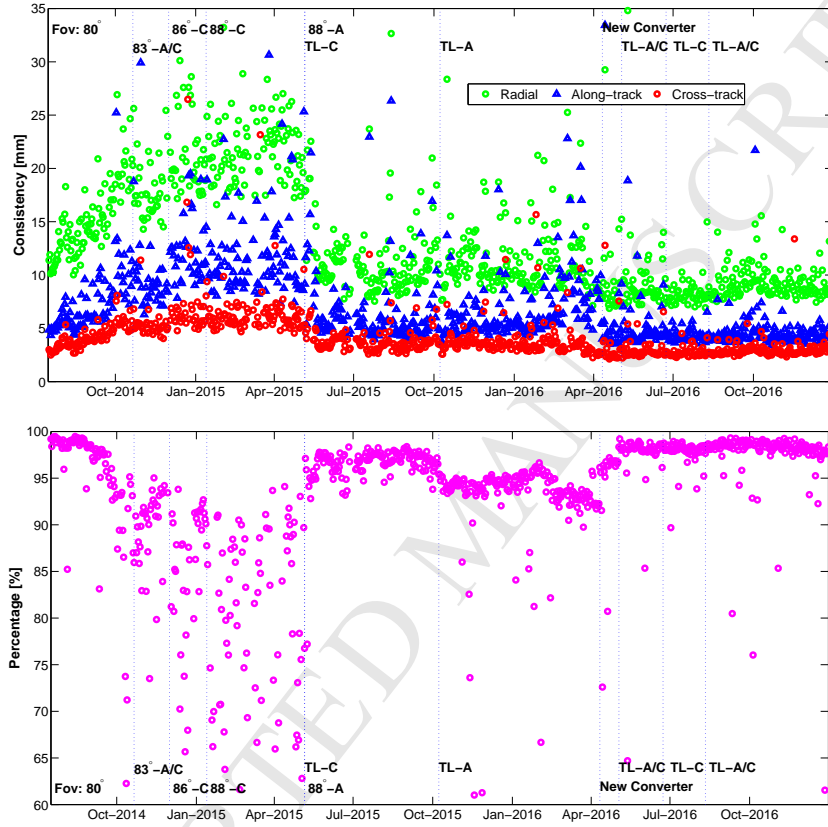
Figure 9: Consistency between kinematic and reduced-dynamic baseline solutions in the radial, along-track and cross-track directions (top), and the percentage of epochs covered by the kinematic solution (bottom) for the full data period.

335   Figure 9 depicts the baseline consistency between the kinematic and reduced-dynamic baselines for the full selected period. The consistency is displayed for Radial, Along-track and Cross-track (R/A/C) direction referring to the Swarm-C coordinates. The baseline consistency is the worst for the radial direction, which can be explained by the geometry (i.e. the associated radial dilution of precision) between GPS satellites and GPS receivers. The baseline consistency

340

20

varies in accordance with the level of carrier phase residual, which is obtained by comparing the modelled carrier phase and the real observations. Lower carrier phase residuals significantly improve the reduced-dynamic and the kinematic PBD. The baseline consistency after implementing the GPS receiver tracking

345 loop modifications and new RINEX converter is at 9.3/4.9/3.0 mm for respectively the R/A/C direction. For around 98.3% of the epochs (5 s time interval), a kinematic baseline solution is available for low ionospheric activity levels. The tracking loop modifications and RINEX converter correction result not only in improved consistency between kinematic and reduced-dynamic PBD, but also

350 an improved stability of the better consistency level.

3.3. Inter-agency comparison

[14] have analyzed the Swarm-A/-C baseline determination for the August 2014 data, which is a month with a relatively low ionospheric activity level. They obtain a kinematic and reduced-dynamic PBD consistency of 40/17/11 mm in

355 the R/A/C directions. In their GHOST baseline determination module, they read one satellite orbit as reference to compute the baseline between two satellites. The mean integer ambiguities fixing success rate achieved by LAMBDA is 93.1%. For the same period, our PBD solutions computed by MODK have better consistency of 14.3/6.6/3.9 mm in the R/A/C directions. The mean am-

360 biguities fixing success rate is 89.7%. Compared to the method in [14] and [7] which rely on the ionosphere-free single-differenced GPS observations, MODK makes use of frequency-dependent GPS observations and ionospheric delay estimates on both frequencies, and therefore obtains better internal consistency between MODK solutions.

365 Another comparison can be done for the period January 2016, as described in [17]. In that paper, two solutions from GSOC and AIUB are compared. GSOC uses the GHOST software package for PBD (marked as *GHOST* in tables). In the research of GSOC, they have created new Swarm RINEX observation files which eliminate the RINEX converter issue on the code observations and all

370 half-cycle ambiguities are corrected to full-cycle values. The AIUB solution is

21

marked as *BSW* which represents the Bernese GNSS software PBD package developed at AIUB. The AIUB baselines are computed in a batch least-squares estimation using DD ionosphere-free GPS observations, and a wide-lane/narrow-lane approach is adopted to fix integer ambiguities [37]. The same batch of corrected GPS RINEX observations [17] is used by AIUB (personal communication with Prof. Adrian Jäggi). However in our research the officially released ESA RINEX files without these corrections, are used. The PBD results for January 2016 data (the first day is excluded due to data gaps) that are available for all three software package solutions, are compared.

Table 3: Consistency between kinematic and reduced-dynamic baseline solutions, kinematic baseline availability and ambiguity fixing success rate for different software packages (consistency unit: [mm], period: January 2016).

Solution	MODK	GHOST	BSW
Radial	0.0+/-11.9	1.3+/-17.9	0.7+/-16.1
Along-track	0.0+/-6.2	-0.1+/-6.0	-0.0+/-6.4
Cross-track	-0.1+/-4.0	0.0+/-5.3	-0.1+/-6.7
Availability	94.5%	73.3%	95.7%
Amb. fix.	72.2%	94.0%	N/A

Table 3 shows the baseline consistency from different research agencies. In general three solutions all have very good internal consistency of 11.9 to 17.9 mm in the vertical direction and a few mm in the horizontal direction. The *MODK* solution has the best agreement of 11.9/6.2/4.0 mm (R/A/C) between the kinematic and reduced-dynamic baselines. *MODK* has in total 94.5% epochs with kinematic solutions, which are computed when there are at least 5 GPS satellites are tracked by both receivers. Both the float ambiguities and the fixed integer ambiguities will be used. Compared with that the *GHOST* solution has 21.2% less availability because the kinematic baselines are computed at epochs when all the integer ambiguities are fixed, and also a minimum of 5 GPS satellites are viewed by two GPS receivers. However, it has to be noted that the *MODK*

22

solution fixes 72.2% ambiguities (note that we have more available epochs). This is lower than the 94.0% from the *GHOST* solutions during January-March 2016, which is reported in [17]. The most important impact factor is that the *GHOST* solution benefits significantly from the correction of the full cycle am-

395 biguities and the RINEX converter issue which increases the code residuals. Unfortunately the *BSW* wide-lane/narrow-lane ambiguity fixing success rate is not available here.

Table 4: Consistency between *MODK* kinematic baseline and reduced-dynamic baseline solutions from different software packages, note that the corrected data is used for all solutions. (unit: [mm], period: 14/15 January 2016).

Solution	Radial	Along-track	Cross-track
MODK	0.1+/-9.0	0.0+/-3.9	-0.1+/-3.1
GHOST	-1.0+/-9.2	1.1+/-6.1	-0.2+/-3.2
BSW	-0.7+/-9.6	0.4+/-6.1	0.1+/-3.2

A new computation is carried out by using two days (14/15 January 2016) of the corrected RINEX files kindly provided by Gerardo Allende-Alba. For

400 the two days, the consistency between *MODK* kinematic and reduced-dynamic baselines is further improved to 9.0/3.9/3.1 mm in the R/A/C directions. More importantly, *MODK* acquires a much higher ambiguities success rate of 97.8% than that of 78.2% when using the un-corrected ESA data (also two days). Other comparisons are done to check the consistency between the *MODK* kine-

405 matic baseline and the *GHOST* and *BSW* reduced-dynamic baselines. The *MODK-GHOST* and *MODK-BSW* baseline consistency have good agreement and are close to the *MODK* kinematic and reduce-dynamic baseline consistency (Table 4). It indicates that the *MODK* solutions are very consistent with the solutions from the GHOST and the Bernese software packages.

410 Another comparison is done for the reduced-dynamic baselines. When we use the ESA data, the R/A/C reduced-dynamic baseline comparison is 4.3/4.3/2.1 mm between *MODK* and *GHOST* solutions, and 3.1/4.3/2.5 mm between *MODK*

and *BSW* solutions (Table 5). However, the *GHOST* and *BSW* solutions have much better agreement of 1.5/1.0/1.4 mm, as they are using the same corrected

415 RINEX files with lower code residuals and full-cycle ambiguities. The lower ambiguities fixing success rate in *MODK* also explains the larger reduced-dynamic baseline differences between *MODK* and *GHOST*. However after the use of same corrected RINEX files in MODK, the results of same comparisons are improved to 1 mm level in three directions, as displayed in Table 5.

Table 5: Inter-agency reduced-dynamic baseline consistency comparison when using different (*MODK* uses ESA data) and same (*MODK* also uses the corrected data) GPS RINEX observations (unit: [mm]).

Solution	Radial	Along-track	Cross-track
ESA data (January 2016)			
MODK-GHOST	0.1+/-4.3	0.6+/-4.3	-0.1+/-2.1
MODK-BSW	-0.2+/-3.1	-0.0+/-4.3	0.0+/-2.5
Corrected data (14/15 January 2016)			
MODK-GHOST	0.2+/-1.5	0.5+/-1.2	-0.0+/-1.1
MODK-BSW	-0.0+/-0.9	-0.1+/-1.0	0.0+/-1.1
GHOST-BSW	-0.3+/-1.5	-0.5+/-1.0	0.1+/-1.4

420 *3.4. Satellite laser ranging validation*

The availability of SLR observations for the Swarm satellites allows an independent validation of the absolute orbit solutions. The SLR system offers an opportunity to assess the accuracy of the GPS-based orbit solutions in the direction of the line-of-sight between the SLR ground stations and the Swarm

425 satellites. In order to eliminate spurious observations, an editing threshold of 50 cm is used, which is more than an order of magnitude above the RMS of fit levels, and observations below the 10° elevation cutoff angle are excluded. A SLR retro-reflector modeling pattern from German Research Center for Geosciences (GFZ) is included [38]. Furthermore seven SLR stations (Kiev, Simeiz,

24

₄₃₀ Arequipa, Borowiec, Changchun, San Fernando, Riga) with large mean offsets are excluded. Ultimately, 83.4% and 86.4% of the SLR observations are used for Swarm-A and -C, respectively. Exactly same SLR validation scheme is used for all different orbit solutions. Table 6 and Figure 10 include the results of comparing the different orbit solutions with the independent SLR observations.

Table 6: Mean and RMS of fit of SLR observations for different orbit solutions of MODK. The ESA solutions are included as reference. (unit: [mm], period: July 2014 - December 2016).

Solution	Swarm-A	Swarm-C
PBD	0.6+/-21.4	-0.7+/-20.7
POD	0.7+/-20.5	-0.7+/-20.3
ESA	2.3+/-19.7	0.6+/-20.2
Obs. No.	51234	49823

₄₃₅ It can be observed that for the MODK POD orbits the RMS of fit of SLR validation is quite close to the orbits from ESA. Note that the ESA orbits are also computed at TU Delft using the original GHOST reduced-dynamic POD tool instead of the MODK tool. For the ESA orbit computation, a batch least-squares method is used and the ionosphere-free combination PCV maps ₄₄₀ are included [12]. The SLR validation statistics confirm that MODK provides high-precision orbit solutions. However, for the PBD solutions the RMS of SLR fit deteriorates by only 1 mm for both Swarm-A and -C. Similar result is reported by [23, 15] that the wrongly fixed integer ambiguities reduce the orbit precision. The fixing process can also be easily influenced by the ionospheric ₄₄₅ activity level between two receivers. More importantly, the code residual level enlarged by errors due to the RINEX converter software issue, also downgrades the float ambiguities estimate accuracy and the subsequent integer ambiguity fixing success rate. There is no such impact on the single-satellite POD which only makes use of float ambiguities.

₄₅₀ Table 7 shows SLR validation is done to different solutions for January 2016
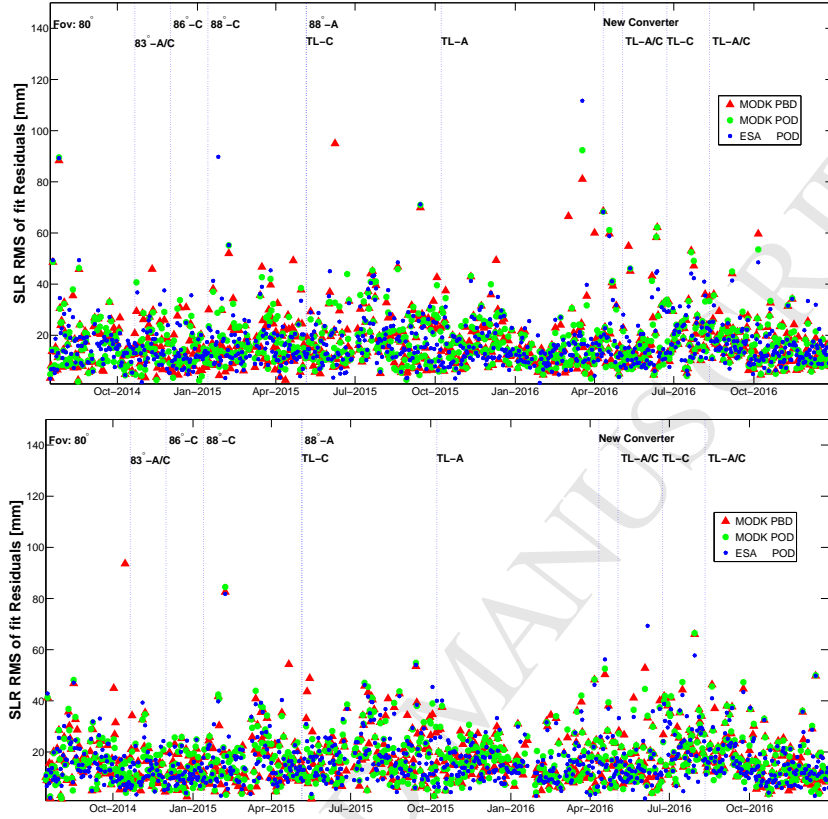
25

Figure 10: The daily RMS of fit of SLR observations for different MODK orbit solutions for Swarm-A (top) and -C (bottom). The ESA solutions are included as reference. (unit: [m], period: July 2014 - December 2016).

data. Unfortunately the number of laser observations of both satellites is low for this month (most observations are from the first half of this month). It can be clearly seen that after using the acceleration constraints in the PBD of *MODK*, the mean SLR validation difference between two satellites decreases from 2.2 (5.8-3.7) to 0.8 (5.1-4.3) mm. This finding corresponds to similar conclusion in [17] which uses a good tracking SLR station -Yarragadee, Australia- to show the better SLR consistency in mean for PBD orbits than POD orbits. More importantly, there is nearly no precision reduction from the *MODK* POD to PBD orbits. It is mainly due to the fact that January 2016 is a month with

26

Table 7: Mean and RMS of fit of SLR observations for different software packages orbit solutions (unit: [mm], period: January-2016).

Software	Solution	Swarm-A	Swarm-C
MODK	PBD	-4.3+/-20.1	-5.1+/-21.1
GHOST	PBD	-3.1+/-19.4	-3.9+/-21.5
BSW	PBD	2.8+/-20.7	2.5+/-22.2
MODK	POD	-3.7+/-19.6	-5.8+/-21.5
ESA	POD	-1.8+/-19.5	-4.5+/-20.6
Obs. No.		910	923

460 lower ionospheric activity, and more importantly the first GPS receiver tracking loop modification further reduces the GPS carrier phase residual level, which is beneficial for the POD and PBD.

4. Summary and discussion

Two pendulum formation flying Swarm -A/-C satellites baseline solutions 465 have been generated for a 30 months data period. The solutions are based on an extended Kalman filter with relative empirical accelerations to constrain the dynamics between satellites. The LAMBDA method is used to fix double-differenced carrier phase ambiguities, where it is not required to fix all ambiguities at a certain epoch. It is possible to fix a subset which acquires the 470 maximum of fixed ambiguities. The LAMBDA method makes use of the float ambiguities and the associated covariance matrices from the Kalman filter. A strict and aggressive validation scheme is adopted to test the fixed integer ambiguities. Moreover, in-flight calibrated frequency-dependent antenna phase and code maps are used to correct the GPS observations. The external SLR val-475 idation confirms that the orbit determination precision obtained in this study reaches a level comparable with the official ESA orbit solutions.

The ionospheric activity level has a big impact on the integer ambiguity

fixing and therefore also the baseline determination. To minimize its impact, a few modifications and a new GPS RINEX converter have been made to the
480 Swarm on-board GPS receivers between 2014 and 2016. These are proved to be effective in many aspects. Firstly, the number of GPS satellites simultaneously tracked by two GPS receivers is influenced by the antenna field of view changes. Larger antenna field of view improves the number of tracked GPS satellites for single receiver, however similar field of view should be guaranteed to have better
485 geometry, or larger number of simultaneously tracked GPS satellites by two receivers. Secondly, the GPS receiver carrier phase tracking performance is clearly influenced by ionospheric scintillations, therefore the downgraded ionospheric activity from 2014 to 2016 significantly reduces the carrier phase residuals and therefore facilitates the baseline determination. The changes of GPS receiver
490 carrier phase tracking loop bandwidth reduces the carrier phase residuals near the geomagnetic equator and poles, especially the first modification which took place during May-October 2015. In addition, the integer ambiguity fixing is affected by the code observation quality. Fixing the RINEX converter software issue on 11 April 2016 results in much lower code residual level, and acquires
495 a stable 90% ambiguity fixing success rate. Finally, the consistency between the kinematic and the reduced-dynamic baseline is determined by the phase residual level and the software issue in the GPS RINEX converter. After all the changes, this research eventually shows a consistency level of 9.3/4.9/3.0 mm in the radial/along-track/cross-track directions, with 98.3% available kinematic
500 baselines.

An inter-agency comparison is done between this research (Delft University of Technology) and the German Space Operations Center (GSOC) solution and the Astronomisches Institut - Universität Bern (AIUB) solution. The January 2016 data is selected for comparison. Our research achieves the best kinematic
505 and reduced-dynamic baseline consistency of 11.9/6.2/4.0 mm in radial/along-track/cross-track directions. When using the same corrected RINEX files (only 14/15 January 2016 data is available) provided by GSOC, the consistency is further improves to 9.0/3.9/3.1 mm. The correction of the RINEX converter

28

software issue and the correction from half-cycle ambiguities to full-cycle ambi-

510 guities indeed help. Reduced-dynamic baselines from different software packages show agreement of 1 mm level in three directions. When comparing our kinematic baselines with the GSOC and AIUB reduced-dynamic baselines, the consistency is close to the consistency between our kinematic and reduced-dynamic solutions. It indicates our baseline solutions agree well with other baseline deter-

515 mination software packages. This precise pendulum Swarm-A and -C kinematic baselines precision level might be very promising for the research to recover the gravity field and its variations.

This research shows that it is important to be aware of the changing quality of the Swarm GPS data, which can be influenced by ionospheric activity and

520 receiver settings. The implemented GPS receiver tracking loop modifications and RINEX converter correction are proved to be working properly to improve the baseline determination between two pendulum formation flying Swarm-A and -C satellites. Future work can be also put on investigating the more dynamic high-low Swarm-B/-A or Swarm-B/-C baselines, for which the baseline

525 determination will be more challenging.

Acknowledgment

29

line solutions. We also acknowledge two anonymous reviewers for reviewing this paper.

540 **References**

[1] E. Friis-Christensen, H. Lühr, G. Hulot, Swarm: A constellation to study the Earths magnetic field, Earth Planets Space 58 (4) (2006) 351–358. `doi:10.1186/BF03351933`.

[2] E. Friis-Christensen, H. Lühr, D. Knudsen, R. Haagmans, Swarm–an Earth 545 observation mission investigating geospace, Adv. Space Res. 41 (1) (2008) 210–216. `doi:10.1016/j.asr.2006.10.008`.

[3] B. D. Tapley, S. Bettadpur, M. Watkins, C. Reigber, The gravity recovery and climate experiment: Mission overview and early results, Geophys. Res. Lett. 31 (9) (2004) L0960. `doi:10.1029/2004GL019920`.

550 [4] G. Krieger, M. Zink, M. Bachmann, B. Bräutigam, D. Schulze, M. Martone, P. Rizzoli, U. Steinbrecher, J. W. Antony, F. De Zan, et al., TanDEM-X: A radar interferometer with two formation-flying satellites, Acta Astronaut. 89 (2013) 83–98. `doi:10.1016/j.actaastro.2013.03.008`.

[5] S. Persson, S. Veldman, P. Bodin, PRISMA-a formation flying project in 555 implementation phase, Acta Astronaut. 65 (9) (2009) 1360–1374. `doi: 10.1016/j.actaastro.2009.03.067`.

[6] S. D'Amico, J.-S. Ardaens, S. De Florio, Autonomous formation flying based on GPS PRISMA flight results, Acta Astronaut. 82 (1) (2013) 69–79. `doi:10.1016/j.actaastro.2012.04.033`.

560 [7] A. Jäggi, C. Dahle, D. Arnold, H. Bock, U. Meyer, G. Beutler, J. van den IJssel, Swarm kinematic orbits and gravity fields from 18months of GPS data, Adv. Space Res. 57 (1) (2016) 218–233. `doi:10.1016/j.asr.2015. 10.035`.

[8] F. Zangerl, F. Griesauer, M. Sust, O. Montenbruck, S. Buchert, A. Garcia,
SWARM GPS precise orbit determination receiver initial in-orbit perfor-
mance evaluation, Proceedings of the 27th International Technical Meeting
of the Satellite Division of the Institute of Navigation (ION-GNSS+-2014),
Tampa, Florida (2014) 1459–1468.

[9] O. Montenbruck, M. Garcia-Fernandez, Y. Yoon, S. Schön, A. Jäggi, An-
tenna phase center calibration for precise positioning of LEO satellites,
GPS Solut. 13 (1) (2009) 23–34. `doi:10.1007/s10291-008-0094-z`.

[10] H. Bock, A. Jäggi, U. Meyer, R. Dach, G. Beutler, Impact of GPS antenna
phase center variations on precise orbits of the GOCE satellite, Adv. Space
Res. 47 (11) (2011) 1885–1893. `doi:10.1016/j.asr.2011.01.017`.

[11] U. Tancredi, A. Renga, M. Grassi, Validation on flight data of a closed-
loop approach for GPS-based relative navigation of LEO satellites, Acta
Astronaut. 86 (2013) 126–135. `doi:10.1016/j.actaastro.2013.01.005`.

[12] J. van den IJssel, J. Encarnação, E. Doornbos, P. Visser, Precise science
orbits for the Swarm satellite constellation, Adv. Space Res. 56 (6) (2015)
1042–1055. `doi:10.1016/j.asr.2015.06.002`.

[13] N. Zehentner, T. Mayer-Gürr, Precise orbit determination based on raw
GPS measurements, J. Geod. 90 (3) (2016) 275–286. `doi:10.1007/`
`s00190-015-0872-7`.

[14] G. Allende-Alba, O. Montenbruck, Robust and precise baseline determina-
tion of distributed spacecraft in LEO, Adv. Space Res. 57 (1) (2016) 46–63.
`doi:10.1016/j.asr.2015.09.034`.

[15] X. Mao, P. Visser, J. van den IJssel, Impact of GPS antenna phase center
and code residual variation maps on orbit and baseline determination of
GRACE, Adv. Space Res. 59 (12) (2017) 2987–3002. `doi:10.1016/j.asr.`
`2017.03.019`.

[16] D. Gu, B. Ju, J. Liu, J. Tu, Enhanced GPS-based GRACE baseline determination by using a new strategy for ambiguity resolution and relative phase center variation corrections, Acta Astronaut. 138 (2017) 176–184. `doi:10.1016/j.actaastro.2017.05.022`.

595 [17] G. Allende-Alba, O. Montenbruck, A. Jäggi, D. Arnold, F. Zangerl, Reduced-dynamic and kinematic baseline determination for the Swarm mission, GPS Solut. 21 (3) (2017) 1275–1284. `doi:10.1007/s10291-017-0611-z`.

[18] S. Buchert, F. Zangerl, M. Sust, M. André, A. Eriksson, J.-E. Wahlund, 600 H. Opgenoorth, SWARM observations of equatorial electron densities and topside GPS track losses, Geophys. Res. Lett. 42 (7) (2015) 2088–2092. `doi:10.1002/2015GL063121`.

[19] C. Xiong, C. Stolle, H. Lühr, The Swarm satellite loss of GPS signal and its relation to ionospheric plasma irregularities, Space Weather 14 (8) (2016) 605 563–577. `doi:10.1002/2016SW001439`.

[20] J. van den IJssel, B. Forte, O. Montenbruck, Impact of Swarm GPS receiver updates on POD performance, Earth Planets Space 68 (1) (2016) 1–17. `doi:10.1186/s40623-016-0459-4`.

[21] C. Dahle, D. Arnold, A. Jäggi, Impact of tracking loop settings of the 610 Swarm GPS receiver on gravity field recovery, Adv. Space Res. 59 (12) (2017) 2843–2854. `doi:10.1016/j.asr.2017.03.003`.

[22] European Space Research and Technology Centre, Swarm Spacecraft Anomalies And Manoeuvers History (till 31 May 2017, PE-RP-ESA-PLSO-0591), Tech. rep., European Space Agency (2017).

615 [23] R. Kroes, O. Montenbruck, W. Bertiger, P. Visser, Precise GRACE baseline determination using GPS, GPS Solut. 9 (1) (2005) 21–31. `doi:10.1007/s10291-004-0123-5`.

[24] P. J. Teunissen, An optimality property of the integer least-squares estimator, J. Geod. 73 (11) (1999) 587–593. doi:10.1007/s001900050269.

[25] P. W. L. van Barneveld, Orbit determination of satellite formations, Ph.D. thesis, Delft University of Technology, ISBN: 9778-94-6191-546-7 (2012).

[26] M. Wermuth, O. Montenbruck, T. Van Helleputte, GPS high precision orbit determination software tools (GHOST), in: Proceedings of 4th International Conference on Astrodynamics Tools and Techniques, Madrid, ESA WPP-308, 2010, pp. 3–6.

[27] T. Mayer-Gürr, D. Rieser, E. Hoeck, J. M. Brockmann, W.-D. Schuh, I. Krasbutter, J. Kusche, S. Maier, S. Krauss, W. Hausleitner, et al., The new combined satellite only model GOCO03s, presented at International Symposium on Gravity, Geoid and Height Systems GGHS 2012, Venice, Italy.

[28] D. D. McCarthy, G. Petit, IERS conventions (2003), Tech. rep., International Earth Rotation And Reference Systems Service (IERS) (Germany), 2004. (2004).

[29] F. Lyard, F. Lefevre, T. Letellier, O. Francis, Modelling the global ocean tides: modern insights from FES2004, Ocean Dynam. 56 (5-6) (2006) 394–415. doi:10.1007/s10236-006-0086-x.

[30] L. G. Jacchia, Thermospheric temperature, density, and composition: new models, SAO special report 375.

[31] L. Prange, E. Orliac, R. Dach, D. Arnold, G. Beutler, S. Schaer, A. Jäggi, CODÉs five-system orbit and clock solutionthe challenges of multi-GNSS data analysis, J. Geod. 91 (4) (2017) 345–360. doi:10.1007/s00190-016-0968-8.

[32] R. Dach, S. Schaer, S. Lutz, M. Meindl, H. Bock, E. Orliac, L. Prange, D. Thaller, L. Mervart, A. Jäggi, et al., Center for Orbit Determination

645   In Europe: IGS Technical Report 2014, Tech. rep., Astronomical Institute,
        University of Bern (2015).

[33]   R. Schmid, R. Dach, X. Collilieux, A. Jäggi, M. Schmitz, F. Dilssner,
        Absolute IGS antenna phase center model igs08. atx: status and po-
        tential improvements, J. Geod. 90 (4) (2016) 343–364. `doi:10.1007/`
650   `s00190-015-0876-3`.

[34]   R. Dach, S. Schaer, D. Arnold, E. Orliac, L. Prange, A. Susnik, A. Villiger,
        A. Jäggi, CODE final product series for the IGS, Tech. rep., Astronomical
        Institute, University of Bern (2016).

[35]   W. Gurtner, L. Estey, RINEX - The Receiver Independent Exchange For-
655   mat (Version 3.02), Tech. rep., International GNSS Service (IGS), RINEX
        Working Group and Radio Technical Commission for Maritime Services
        Special Committee 104 (RTCM-SC104) (2013).

[36]   A. Jäggi, R. Dach, O. Montenbruck, U. Hugentobler, H. Bock, G. Beutler,
        Phase center modeling for LEO GPS receiver antennas and its impact on
660   precise orbit determination, J. Geod. 83 (12) (2009) 1145–1162. `doi:10.`
        `1007/s00190-009-0333-2`.

[37]   A. Jäggi, U. Hugentobler, H. Bock, G. Beutler, Precise orbit determina-
        tion for GRACE using undifferenced or doubly differenced GPS data, Adv.
        Space Res. 39 (10) (2007) 1612–1619. `doi:10.1016/j.asr.2007.03.012`.

665 [38] R. Neubert, L. Grunwaldt, J. Neubert, The retro-reflector for the CHAMP
        satellite: Final design and realization, in: Proceedings of the 11th Interna-
        tional Workshop on Laser Ranging, 1998, pp. 260–270.
        URL `http://ilrs.gsfc.nasa.gov/docs/rra_champ.pdf,LastAccess:`
        `05/Dec/2017`.

34

The analysis of 30 months data for the Swarm constellation.

The influence of changing ionospheric activity is analyzed.

GPS receiver modifications improve baseline determination.

The corrected GPS data obtains better baseline precision.

Inter-agency comparison shows good agreement.